

Density-Dependent Synthetic Gauge Fields Using Periodically Modulated Interactions

S. Greschner,¹ G. Sun,¹ D. Poletti,^{2,3} and L. Santos¹

¹*Institut für Theoretische Physik, Leibniz Universität Hannover, Appelstr. 2, DE-30167 Hannover, Germany*

²*Engineering Product Development, Singapore University of Technology and Design, 20 Dover Drive, 138682 Singapore*

³*Merlion MajuLab, CNRS-UNS-NUS-NTU International Joint Research Unit, UMI 3654, Singapore*

We show that density-dependent synthetic gauge fields may be engineered by combining periodically modulated interactions and Raman-assisted hopping in spin-dependent optical lattices. These fields lead to a density-dependent shift of the momentum distribution, may induce superfluid-to-Mott insulator transitions, and strongly modify correlations in the superfluid regime. We show that the interplay between the created gauge field and the broken sublattice symmetry results, as well, in an intriguing behavior at vanishing interactions, characterized by the appearance of a fractional Mott insulator.

The emulation of synthetic electromagnetism in cold neutral gases has attracted a major interest [1, 2]. Artificial electric and magnetic fields have been induced using lasers [3–5]. Moreover, these setups may be extended to generate non-Abelian fields, and in particular spin-orbit coupling [6–13]. Synthetic fields may be generated as well in optical lattices, and recent experiments have created artificial staggered [14–16] and uniform [17, 18] magnetic fields. These fields are however static, as they are not influenced by the atoms.

The dynamical feedback between matter and gauge fields plays, however, an important role in various areas of physics, ranging from condensed-matter [19] to quantum chromodynamics [20], and its realization in cold lattice gases is attracting a growing attention [21]. Schemes have been recently proposed for multi-component lattice gases, such that the low-energy description of these systems is that of relevant quantum field theories [22–31]. The back-action of the atoms on the value of a synthetic gauge field is expected to lead to interesting physics, including statistically-induced phase transitions and anyons in 1D lattices [32], and chiral solitons in Bose-Einstein condensates [33].

Periodically modulated optical lattices open interesting possibilities for the engineering of lattice gases [16–18, 34–40]. In particular, periodic lattice shaking results in a modified hopping rate [34–36], which has been employed to drive the superfluid (SF) to Mott insulator (MI) transition [37], to simulate frustrated classical magnetism [38], and to create tunable gauge potentials [16]. Interestingly, a periodically modulated magnetic field may be employed in the vicinity of a Feshbach resonance to induce periodically modulated interactions, which result in a non-linear hopping rate that depends on the occupation differences at neighboring sites [41–43].

In this Letter, we show that combining periodic interactions and Raman-assisted hopping may induce a density-dependent gauge field in 1D lattices. The created field results in a density-dependent shift of the momentum distribution that may be probed in time-of-flight (TOF) experiments. Moreover, contrary to the Peierls phase induced in shaken lattices [16], the created field cannot be gauged out, and hence affects significantly the ground-state properties of the lattice gas, leading to gauge-induced SF to MI transitions, the emergence of MI at vanishing interaction, and strongly modified

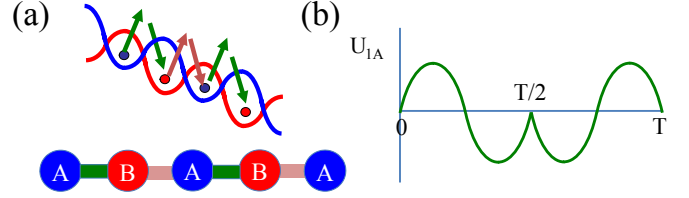


FIG. 1: (Color online) Scheme of the AB set up: (a) for $0 < t < T/2$ Raman assisted hopping couples an A site with the B site at their right; for $T/2 < t < T$ it couples an A site with the B site at their left; (b) the $U_{A1}(t)$ function is $\sin(\omega_{AB}t)$ for $0 < t < T/2$ and $-\sin(\omega_{AB}t)$ for $T/2 < t < T$, with $\omega_{AB} = 4\pi/T$.

correlations in the SF regime.

AB model. – We introduce in the following a possible set-up that creates a density-dependent Peierls phase that cannot be gauged out. We consider a tilted 1D spin-dependent lattice (see Fig. 1), in which atoms in state $|1\rangle$ ($|2\rangle$) are confined in the sublattice A (B). A first pair of Raman lasers induces Raman-assisted hopping between an A site and the B site to its right, whereas a second pair leads to hopping between an A site and the B site to its left [44]. We consider that within a period T , for $0 < t < T/2$ the Raman assisted coupling AB (BA) is on (off) and vice versa for $T/2 < t < T$. The Hamiltonian of the system is:

$$\hat{H}^{AB} = - \sum_j \left[J_{AB}(t) \hat{b}_{2j}^\dagger \hat{b}_{2j+1} + J_{BA}(t) \hat{b}_{2j}^\dagger \hat{b}_{2j-1} + \text{h.c.} \right] + \frac{U_A(t)}{2} \sum_j \hat{n}_{2j}(\hat{n}_{2j} - 1) + \frac{U_B}{2} \sum_j \hat{n}_{2j+1}(\hat{n}_{2j+1} - 1). \quad (1)$$

where $J_{AB} = J$ and $J_{BA} = 0$ for $0 < t < T/2$, $J_{AB} = 0$ and $J_{BA} = J$ for $T/2 < t < T$, and even (odd) site index corresponds to the A (B) sublattice. We consider that the interaction of components $|1\rangle$ can be independently modulated from those of $|2\rangle$, such that $U_A = U_{A0} + U_{A1}(t)$, with $U_{A1}(t) = U_{A1}(t+T)$ and $\int_t^{t+T} dt' U_{A1}(t') = 0$, whereas U_B is constant (we consider for simplicity $U_{A0} = U_B \equiv U$ [45]). As shown in Refs. [41, 42] a sufficiently fast modulation of the interactions leads to an effective model with a density-dependent hopping (as discussed in the Supplemen-

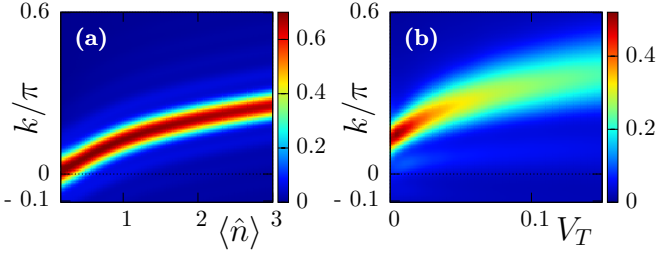


FIG. 2: (Color online) (a) Ground-state quasi-momentum distribution for model (2) for an homogeneous distribution in 24 sites with $\Omega_{AB} = \pi/4$, $U = 0.2J$, and a density $\langle \hat{n} \rangle$; (b) same for a harmonically trapped gas as a function of V_T (see text) for $\Omega_{AB} = \pi/4$, $U = J$ and 24 particles in 24 sites. Both figures show density-matrix renormalization group (DMRG) [48] results with 500 states, and a maximal occupation per site $n_{max} = 10$.

tal Material [46], just modulating the interactions in a standard Bose-Hubbard model does result in a density-dependent Peierls phase, but this phase can be gauged out [46]). For the particular case of the AB model we obtain for a fast modulation the effective Hamiltonian [47]:

$$\hat{H}_{\text{eff}}^{AB} = -\sum_j \left[\hat{b}_{2j}^\dagger \tilde{J}_{AB}(\hat{n}_{2j}) \hat{b}_{2j+1} + \hat{b}_{2j}^\dagger \tilde{J}_{BA}(\hat{n}_{2j}) \hat{b}_{2j-1} + \text{h.c.} \right] + \frac{U}{2} \sum_j \hat{n}_{2j}(\hat{n}_{2j}-1) + \frac{U}{2} \sum_j \hat{n}_{2j+1}(\hat{n}_{2j+1}-1), \quad (2)$$

with $\tilde{J}_{AB}(\hat{n}_{2j}) = \frac{J}{T} \int_0^{T/2} dt e^{iV(t)\hat{n}_{2j}/\hbar}$, $\tilde{J}_{BA}(\hat{n}_{2j}) = \frac{J}{T} \int_0^{T/2} dt e^{iV(t+T/2)\hat{n}_{2j}/\hbar}$, and $V(t) = \int_0^t U_{A1}(t') dt'$.

For $U_{A1}(t) = \tilde{U}_{A1} \sin(\omega_{AB}t)$ for $0 < t < T/2$ (with $\omega_{AB} = 4\pi/T$), and $U_{A1}(t) = -\tilde{U}_{A1} \sin(\omega_{AB}t)$ for $T/2 < t < T$ (see Fig. 1(b)), $\tilde{J}_{AB}(\hat{n}_{2j}) = \frac{J}{2} J_0(\Omega_{AB} \hat{n}_{2j}) e^{i\Omega_{AB} \hat{n}_{2j}}$, whereas $\tilde{J}_{BA}(\hat{n}_{2j}) = \tilde{J}_{AB}(\hat{n}_{2j})^*$, with $\Omega_{AB} = \tilde{U}_{A1}/\hbar\omega_{AB}$. For more general forms of $U_{A1}(t)$ [46], $\arg[\tilde{J}_{AB}] = \phi_{AB}\hat{n}_{2j}$ and $\arg[\tilde{J}_{BA}] = \phi_{BA}\hat{n}_{2j}$. The created Peierls phase cannot be gauged out if $\Phi \equiv \phi_{AB} - \phi_{BA} \neq 0$, crucially altering the ground-state properties.

Quasi-momentum distribution.— The created Peierls phase results in a drift of the quasi-momentum distribution in the SF regime. As in recent experiments on shaken lattices [16], this shift may be probed in TOF (details about experimental detection are discussed below). Fig. 2(a) shows the quasi-momentum distribution as a function of the average density $\langle \hat{n} \rangle$ for an homogeneous system with $\Omega_{AB} = \pi/4$ and $U = 0.2J$. However, in contrast to shaken lattice experiments, the momentum shift is density dependent. This dependence results in a non-trivial behavior of the quasi-momentum distribution in the presence of an external harmonic confinement, which may be accounted for by an additional term $V_T \sum_j (j - L/2)^2 \hat{n}_j$ in the Hamiltonian (2). As shown in Fig. 2(b), for larger V_T the quasi-momentum distribution shifts due to growing central density, and broadens due to the inhomogeneous density distribution $\langle \hat{n}_j \rangle$.

Ground-state phase diagram.— The non-gaugeable density-dependent Peierls phase and the associated broken AB symmetry are crucial for the ground-state physics of the AB model (see Fig. 3 in which μ is the chemical potential). MI phases at half-integer filling are induced by the AB asymmetry, opening immediately at any finite J . For $\langle \hat{n} \rangle = 1/2$ at $J/U \ll 1$ we may project on the manifold with 0 or 1 particle per site and we may identify $|0\rangle \rightarrow |\uparrow\rangle$ and $|1\rangle \rightarrow |\downarrow\rangle$, obtaining up to $\mathcal{O}(J^2/U)$ the effective spin- $\frac{1}{2}$ Hamiltonian $\hat{H}_{1/2} = \hat{H}_0 + \hat{H}_2$, with $\hat{H}_0 = -J \sum_j \hat{S}_j^+ \hat{S}_{j+1}^- + \text{h.c.}$, and $(U/J^2)\hat{H}_2 = \sum_j [\hat{S}_{2j}^+ (\frac{1}{2} + \hat{S}_{2j+1}^z) \hat{S}_{2j+2}^- + \Gamma^2 \hat{S}_{2j-1}^+ (\frac{1}{2} + \hat{S}_{2j}^z) \hat{S}_{2j+1}^- + \text{h.c.}] - (1 + |\Gamma|^2) \sum_j \hat{S}_j^z \hat{S}_{j+1}^z$, with $\Gamma \equiv \frac{1}{2} J_0(\Omega_{AB}) e^{i\Phi/2}$. Hence the perturbative corrections result in nearest neighbor interactions and staggered correlated hopping. Following similar arguments as those employed for the treatment of the spin-Peierls problem [49], one may show that the staggered correlated hopping becomes immediately relevant (in the renormalization group sense) for free hard-core particles, and hence any AB-dependent Γ opens a (band insulator) gapped phase at half-filling for $U \rightarrow \infty$ (see Supplemental Material [46] for details). A similar reasoning applies for higher half-integer fillings $\bar{n} + 1/2$, by considering hard-core particles on top of a pseudo-vacuum with \bar{n} particles per site. Note that the Mott boundaries depend on Φ and hence varying Φ at constant J/U results in gauge-induced phase transitions (Fig. 3(b)), similar as the statistical transitions of Ref. [32]. In particular, for $\Phi \rightarrow \pi$ one observes a strong enhancement of the MI gaps. Half-integer and integer MI may be revealed by the appearance of density plateaus in the presence of a harmonic trap [50].

Vanishing on-site interaction.— The effect of the density-dependent hopping is particularly relevant in the regime of vanishing interaction, $U/J \rightarrow 0$. In this regime, for the usual Hubbard model, the system becomes unstable for $\mu > -J$, i.e. any filling factor becomes possible (note the bunching of curves of constant filling for $\Omega_{AB} = 0$ in Fig. 3(c)). The presence of density-dependent hopping stabilizes the system at low fillings (Fig. 3(c)). Moreover, the AB asymmetry results in a MI at half-filling even for $U/J = 0$. This anomalous behavior results from the effective repulsive character of the gas even when $U = 0$. This may be understood from the two-particle problem, which provides a useful description in the dilute limit [51]. The effective scattering length (in lattice spacing units) becomes of the form [46]:

$$a(U \rightarrow 0) = \frac{[3 + 5 \cos(\Phi)] |\Gamma|^2 + 2}{[5 + 3 \cos(\Phi)] |\Gamma|^2 - 2}, \quad (3)$$

By comparison to a 1D Bose gas of particles with mass m and contact-interaction one may extract an effective interaction strength $g = -2/(am)$ [51]. The scattering length diverges for $|\Gamma| \rightarrow 1/2$, $\Phi \rightarrow 0, 2\pi$ but remains finite and negative for any other phase Φ which coincides with the observation that the AB-correlated hopping Hubbard model behaves as a repulsively interacting system for small filling even in the

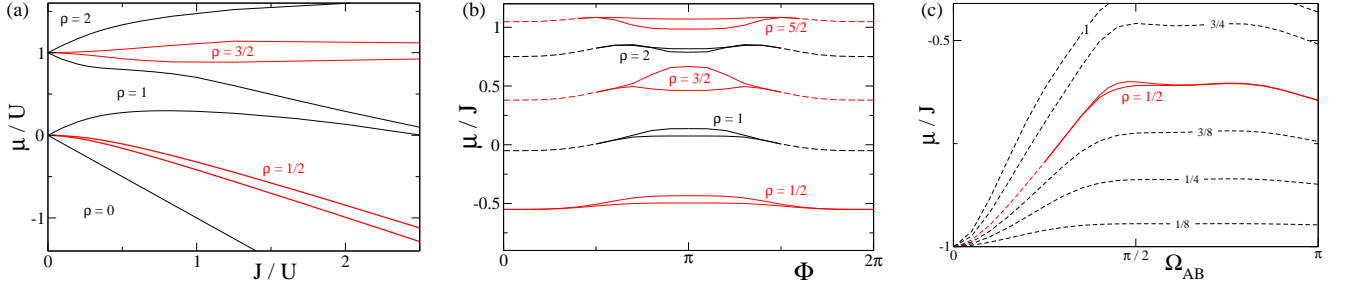


FIG. 3: (Color online) Mott phases at half-integer and integer fillings of model (2). (a) MI-lobes for $\Omega_{AB} = \pi/2$, $\Phi = \pi$. (b) Varying the relative phase Φ may induce phase transitions in the ground state. Here we choose $\Omega_{AB} = \pi/2$ and change Φ [46] for $J/U = 2$ (dashed lines indicate a closing gap) (c) Lines of constant density and MI phase at half-filling for vanishing on-site interactions $U = 0$. In the DMRG-calculation system size L and maximal occupation number of bosons per site n_{max} have been scaled carefully (up to $n_{max} = 12$ and $L = 144$ sites) till a convergence was reached.

limit of $U \rightarrow 0$. Incidentally, we would like to mention that this effect may be observed as well for the anyon model of Ref. [32], although in that case the Mott plateau at half-filling is absent.

Correlation functions in the superfluid regime.— The density-dependent gauge has important consequences for the correlations in the SF regime [46]. This is best understood by employing bosonization [49]: $\hat{b}_j^\dagger \rightarrow \sqrt{\rho(x_j)} e^{-i(\theta(x_j) - \eta x_j)}$, with $\rho(x) = \rho_0 - \frac{1}{\pi} \nabla \phi(x) + \rho_0 \sum_{p \neq 0} e^{i2p(\pi\rho_0 + \phi(x))}$, ρ_0 the average density, and x_j the position of site j . The fields $\theta(x)$ and $\phi(x)$ characterize the density and phase, respectively, whereas η is for a global gaugeable phase shift. The bosonized Hamiltonian acquires the form [46]:

$$\hat{H} = \frac{u}{2\pi} \int dx [K^{-1}(\partial_x \phi)^2 + K(\partial_x \theta)^2 + 2\gamma(\partial_x \phi)(\partial_x \theta)], \quad (4)$$

where u is a velocity, K is the Luttinger parameter, and γ characterizes a mixing term that stems from the density-dependent Peierls phase. The decay of single particle correlations depends only on K as $\langle \hat{b}_i^\dagger \hat{b}_j \rangle \propto |i - j|^{-1/2K}$ [46]. As depicted in Fig. 4, K decreases with increasing Ω_{AB} . This behavior can be understood already from the weak-coupling regime, in which K may be determined analytically [46]:

$$K^2 = \frac{\pi^2 \rho_0 \tilde{F}(\rho_0)}{\frac{2U}{J} - \mathcal{R} \left(\rho_0 \frac{d^2 \tilde{F}}{d\rho^2}(\rho_0) + 2 \frac{d\tilde{F}}{d\rho}(\rho_0) \right)} \quad (5)$$

with \mathcal{R} the real part, $\tilde{F}(\rho) = F(\rho) e^{-i \arg(F(\rho))}$, and $F(\rho) = J_0(\Omega_{AB} \rho) e^{i\Omega_{AB} \rho}$ for the AB model (but the result may be generally applied to other forms of density-dependent tunneling, $F(\hat{n}_j)$). Figure 4 shows that our DMRG results are in excellent agreement with Eq. (5) for small Ω_{AB} , which corresponds to the weak-coupling limit. The reduction of K results on one hand from the trivial reduction of the hopping strength ($J \rightarrow J\tilde{F}(\rho_0)$), and on the other from a non-trivial contribution due to the density dependence (denominator of K). The latter stems from the effective repulsion discussed above. Note in particular, that a density-dependent Peierls

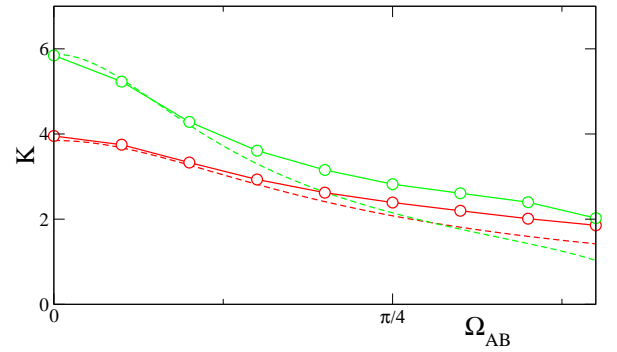


FIG. 4: (Color online) Behavior of the Luttinger parameter K as a function of Ω_{AB} for $U = J/2$ for $\rho_0 = 1.75$ (upper curves) and $\rho_0 = 0.75$ (lower curves). Dashed lines indicate the analytical estimation (5) in the weakly-interacting regime, whereas the circles denote our results from DMRG calculations of the single-particle correlation function.

phase, with $|F(\rho)| = 1$, as that of Ref. [32], would lead as well to strongly modified correlations characterized by a significant reduction of K [46]. The modification of K due to the density-dependent gauge may be directly probed by monitoring the form of the central momentum peak [52].

Adiabatic preparation.— We have focused above on the effective model (2). As for shaken lattices [53], one may start from the ground-state without modulated interactions, and adiabatically increase \tilde{U}_{A1} . We have studied this preparation by means of time-evolving block decimation (TEBD) [54] simulations of the dynamics of Eq. (1) when applying a linear ramp $\tilde{U}_{A1}(t) = \frac{t}{\tau} \tilde{U}_{A1}$ for $t < \tau$, and constant afterwards [46]. Fig. 5 depicts the value k_{max} at which the momentum distribution is maximal, showing that the evolved momentum distribution is in very good agreement with that of the effective model. Note that the drift k_{max} is only linear with $\Omega_{AB} \langle \hat{n} \rangle$ for a sufficiently small value of $\Omega_{AB} \langle \hat{n} \rangle$. For larger $\Omega_{AB} \langle \hat{n} \rangle$ it presents a non-trivial density dependence, especially at low $\langle \hat{n} \rangle$, due to number fluctuations.

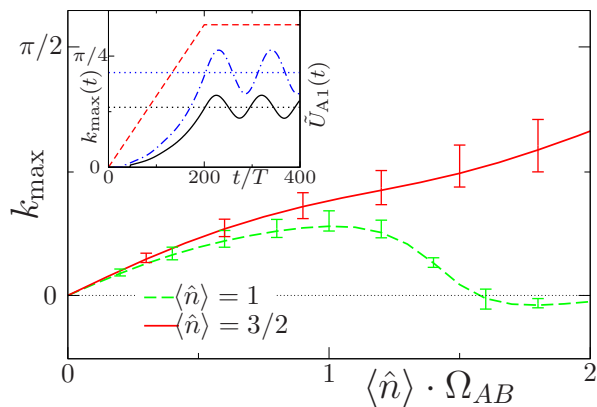


FIG. 5: (Color online) Quasi-momentum k_{max} at which the quasi-momentum distribution of the B sublattice is maximal as a function of $\Omega_{AB}\langle\hat{n}\rangle$ for $\omega = 20J$ and $U = J$. Solid (dashed) lines denote the results obtained from the effective model (2) with $\langle\hat{n}\rangle = 3/2$ (1). The error bars denote the uncertainty (time average and standard deviation for $200 < t/T < 400$) of $k_{max}(t)$ for the case of a linear ramp of \tilde{U}_{A1} with a ramp time of $\tau = 200T$ (see text). (inset) Solid and dash-dotted lines show $k_{max}(t)$ for $\langle\hat{n}\rangle = 3/2$ with $\Omega_{AB} = 0.4$ and 0.8 , whereas the dotted line indicates the value of k_{max} for the effective model (2). We depict with a dashed line the ramp $\tilde{U}_{A1}(t)$.

Detection.— Whereas the density distribution of the effective model corresponds to that measured in the laboratory frame, the measurement of the momentum distribution in TOF presents some features that differ significantly from the shaken lattice case [16]. First, since the lattice is not actually shaken, the overall momentum envelope resulting from the Fourier transform of the Wannier functions does not oscillate in time. Second, whereas the momentum distribution of the B sublattice measured in TOF corresponds to that of the effective model, the distribution of the A sublattice just coincides with that of the effective model (and also with that of the sublattice B) when $V(t) = 0$. For intermediate times, the phase appearing in the conversion between both reference frames leads to a broadening, and eventual blurring, of the TOF peaks [46].

Outlook.— Periodic interactions combined with Raman-assisted hopping may create a density-dependent Peierls phase that results in non-trivial ground-state properties, characterized by a density-dependent momentum distribution, gauge-induced SF to MI transitions, the stabilization of the Hubbard model at vanishing interactions, and modified correlations in the SF phase. Although our discussion has focused on the specific case of the AB model, these peculiar properties are general for all models with a density-dependent Peierls phase [55] (in the Supplemental Material [46] we comment on the case of the anyonic model of Ref. [32]).

The AB model may be extended to create a density-dependent gauge field in a square lattice, in which each row is an exact copy of the AB lattice as that discussed above, and rows are coupled by direct (not Raman-assisted) hops. Tilting the lattice, leads to a row-dependent $\langle\hat{n}\rangle$, and hence to a

different Peierls phase at each row when modulating the interactions. In this way a finite flux may be produced in each plaquette, proportional to the density difference between neighboring rows. As a result, density dependent synthetic magnetic fields may be created, opening interesting possibilities that deserve further investigation.

Acknowledgements.— We thank C. de Morais Smith, M. Di Liberto, M. Dalmonte, A. Eckardt, and U. Schneider for enlightening discussions. We acknowledge support by the cluster of excellence QUEST, the DFG Research Training Group 1729, and the SUTD start-up grant (SRG-EPD-2012-045).

-
- [1] J. Dalibard, F. Gerbier, G. Juzeliunas, and P. Öhberg, *Rev. Mod. Phys.* **83**, 1523 (2011).
 - [2] N. Goldman, G. Juzeliunas, P. Öhberg and I. B. Spielman, arXiv:1308.6533.
 - [3] Y. J. Lin *et al.*, *Phys. Rev. Lett.* **102**, 130401 (2009).
 - [4] Y. J. Lin *et al.*, *Nature* **462**, 628 (2009).
 - [5] Y. J. Lin *et al.*, *Nature Physics* **7**, 531 (2011).
 - [6] Y. J. Lin, K. Jiménez-García and I. B. Spielman, *Nature Physics* **471**, 83 (2011).
 - [7] P. Wang *et al.*, *Phys. Rev. Lett.* **109**, 095301 (2012).
 - [8] L. W. Cheuk *et al.*, *Phys. Rev. Lett.* **109**, 095302 (2012).
 - [9] J. Y. Zhang *et al.*, *Phys. Lett. Lett.* **109**, 115301 (2012).
 - [10] Z. Fu *et al.* *Nat. Phys.* **10**, 110 (2014).
 - [11] L. Zhang *et al.*, *Phys. Rev. A* **87**, 011601(R) (2013).
 - [12] C. Qu, C. Hamner, M. Gong, C. Zhang and P. Engels, *Phys. Rev. A* **88**, 021604(R) (2013).
 - [13] L. J. LeBlanc *et al.*, *New. J. Phys.* **15**, 073011(2013).
 - [14] M. Aidelsburger *et al.* *Phys. Rev. Lett.* **107**, 255301 (2011).
 - [15] K. Jiménez-García *et al.*, *Phys. Rev. Lett.* **108**, 225303 (2012).
 - [16] J. Struck *et al.*, *Phys. Rev. Lett.* **108**, 225304 (2012).
 - [17] M. Aidelsburger *et al.*, *Phys. Rev. Lett.* **111**, 185301 (2013).
 - [18] H. Miyake, G.A. Siviloglou, C.J. Kennedy, W.C. Burton and W. Ketterle, *Phys. Rev. Lett.* **111**, 185302 (2013).
 - [19] M. Levin and X. G. Wen, *Rev. Mod. Phys.* **77**, 871 (2005).
 - [20] J. Kogut, *Rev. Mod. Phys.* **55**, 775 (1983).
 - [21] U. J. Wiese, arXiv:1305.1602.
 - [22] J. I. Cirac, P. Maraner, and J. K. Pachos, *Phys. Rev. Lett.* **105**, 190403 (2010).
 - [23] E. Zohar and B. Reznik, *Phys. Rev. Lett.* **107**, 275301 (2011).
 - [24] E. Kapit and E. Mueller, *Phys. Rev. A* **83**, 033625 (2011).
 - [25] E. Zohar, J. I. Cirac, and B. Reznik, *Phys. Rev. Lett.* **109**, 125302 (2012).
 - [26] D. Banerjee *et al.*, *Phys. Rev. Lett.* **109**, 175302 (2012).
 - [27] L. Tagliacozzo, A. Celi, P. Orland, and M. Lewenstein, *Nat. Commun.* **4**, 2615 (2013).
 - [28] E. Zohar, J. I. Cirac, and B. Reznik, *Phys. Rev. Lett.* **110**, 055302 (2013).
 - [29] D. Banerjee *et al.*, *Phys. Rev. Lett.* **110**, 125303 (2013).
 - [30] E. Zohar, J. I. Cirac, and B. Reznik, *Phys. Rev. Lett.* **110**, 125304 (2013).
 - [31] L. Tagliacozzo, A. Celi, P. Orland, M. W. Mitchell, and M. Lewenstein, *Nat. Commun.* **4**, 2615 (2013).
 - [32] T. Keilmann, S. Lanzmich, I. McCulloch, and M. Roncaglia, *Nat. Commun.* **2**, 361 (2011).
 - [33] M.J. Edmonds, M. Valiente, G. Juzeliunas, L. Santos and P. Öhberg, *Phys. Rev. Lett.* **110**, 085301 (2013).
 - [34] A. Eckardt, C. Weiss, and M. Holthaus, *Phys. Rev. Lett.* **95**,

- 260404 (2005).
- [35] H. Lignier, *et al.*, Phys. Rev. Lett. **99**, 220403 (2007).
- [36] E. Kierig, U. Schnorrberger, A. Schietinger, J. Tomkovic and M.K. Oberthaler, Phys. Rev. Lett. **100**, 190405 (2008).
- [37] A. Zenesini, H. Lignier, D. Ciampini, O. Morsch and E. Arimondo, Phys. Rev. Lett. **102**, 100403 (2009).
- [38] J. Struck *et al.*, Science **333**, 996 (2011).
- [39] Y.-A. Chen *et al.*, Phys. Rev. Lett. **107**, 210405 (2011).
- [40] R. Ma *et al.*, Phys. Rev. Lett. **107**, 095301 (2011).
- [41] J. Gong, L. Morales-Molina and P. Hänggi, Phys. Rev. Lett. **103**, 133002 (2009).
- [42] Á. Rapp, X. Deng, and L. Santos, Phys. Rev. Lett. **109**, 203005 (2012).
- [43] M. Di Liberto, C. E. Creffield, G. I. Japaridze, and C. Morais Smith, Phys. Rev. A **89**, 013624 (2014).
- [44] The laser arrangement is basically the same as that of [D. Jaksch and P. Zoller, New. J. Phys. **5**, 56 (2003)] proposed for the creation of a synthetic (static) magnetic field. However, here we do not demand a spatial dependence of the Rabi frequencies and the AB and BA lasers are switched on and off. The tilting must be sufficiently large to be resolved by the two different Raman pairs. The tilting must be also larger than the Raman-induced hopping rate and the interaction energy. Note also that the tilting should be chosen avoiding photon-assisted resonances [C. Sias *et al.*, Phys. Rev. Lett. **100**, 040404 (2008)], which could result in a significant BA hopping even during the AB pulses.
- [45] An even more intriguing phase space could emerge from assuming $U_{A0} \neq U_B$, however this goes beyond the scope of this current article.
- [46] See the Supplemental Material for details on periodically modulated interactions, the strongly-interacting limit, the calculation of the scattering length for vanishing interaction, time of flight imaging, correlation functions in the SF regime, and the numerical simulations.
- [47] The AB model resembles the anyon model of Ref. [32], in which the inter-site hopping depends on the occupation of the left site. The model of Ref. [32] requires twice as many Raman lasers as the maximal occupation per site, and on-site interactions larger than the laser linewidth. The AB model works with only one laser pair, and for interaction shifts smaller than the laser linewidth (for $\langle \hat{n} \rangle = 5$ and $U = 0.2J$, the linewidth required must be larger than $U \langle \hat{n} \rangle = J$; for J of the order of tens of Hz this is a realistic assumption for typical linewidths [18]). The AB model may be recast as an anyon model without Peierls phase by defining $\hat{a}_{2j} = e^{i\Omega_{AB} \sum_{l < j} \hat{n}_{2l}} \hat{b}_{2j}$, and $\hat{a}_{2j+1} = e^{i\Omega_{AB} \sum_{l \leq j} \hat{n}_{2l}} \hat{b}_{2j+1}$, where the \hat{a} operators fulfill, for $j' > j$, $e^{i\Omega_{AB}} \hat{a}_{2j}^\dagger \hat{a}_{2j'} = \hat{a}_{2j'} \hat{a}_{2j}^\dagger$, $e^{i\Omega_{AB}} \hat{a}_{2j}^\dagger \hat{a}_{2j'+1} = \hat{a}_{2j'+1} \hat{a}_{2j}^\dagger$, $\hat{a}_{2j+1}^\dagger \hat{a}_{2j'+1} = \hat{a}_{2j'+1} \hat{a}_{2j+1}^\dagger$.
- [48] U. Schollwöck, Annals of Physics **326**, 96 (2011).
- [49] Th. Giamarchi, *Quantum Physics in One Dimension*, (Oxford University Press, New York, 2004).
- [50] J. Sherson *et al.*, Nature **467**, bf 68 (2010).
- [51] A. K. Kolezhuk, F. Heidrich-Meisner, S. Greschner and T. Vekua, Phys. Rev B **85**, 064420 (2012).
- [52] B. Paredes *et al.*, Nature **429**, 277 (2004).
- [53] D. Poletti and C. Kollath, Phys. Rev. A **84**, 013615 (2011).
- [54] A. J. Daley, C. Kollath, U. Schollwöck, and G. Vidal, J. Stat. Mech. (2004) P04005.
- [55] Only the half-integer MI and the MI at vanishing interactions demand necessarily the AB asymmetry specific of the AB model.

Supplementary material to

“Density dependent synthetic gauge fields using periodically modulated interactions”

S. Greschner,¹ G. Sun,¹ D. Poletti,² and L. Santos¹¹*Institut für Theoretische Physik, Leibniz Universität Hannover, Appelstr. 2, DE-30167 Hannover, Germany*²*Engineering Product Development, Singapore University of Technology and Design, 20 Dover Drive, 138682 Singapore*

In this supplementary material, we provide additional details on the periodically modulated interactions, the strongly-interacting limit, the calculation of the scattering length of the AB-model, some aspects of the time of flight (TOF) imaging, correlation functions in the presence of density-dependent hopping, and the numerical simulation of real-time evolutions.

A. SINGLE-COMPONENT BOSE-HUBBARD HAMILTONIAN WITH PERIODICALLY MODULATED INTERACTIONS

We consider in this section single-component bosons in a 1D optical lattice with periodically modulated short-range interactions. Considering a large-enough gap between the first two Bloch bands, we may restrict the description of the system to a single band Bose-Hubbard Hamiltonian:

$$\hat{H}(t) = -J \sum_{\langle ij \rangle} \hat{b}_i^\dagger \hat{b}_j + \frac{U_0 + U_1(t)}{2} \sum_i \hat{n}_i (\hat{n}_i - 1), \quad (1)$$

where \hat{b}_i is the bosonic annihilation operator at site i , $\hat{n}_i = \hat{b}_i^\dagger \hat{b}_i$, $J > 0$ is the hopping rate, $\langle \dots \rangle$ denotes nearest neighbors, $U_1(t) = U_1(t+T)$, and $\int_t^{t+T} dt' U_1(t') = 0$.

We perform the transformation $|\psi'(t)\rangle = \hat{R}(t)|\psi(t)\rangle$, with $\hat{R}(t) = e^{i\frac{V(t)}{2} \sum_j \hat{n}_j (\hat{n}_j - 1)}$, such that $\frac{d}{dt} V(t) = U_1(t)$ (note that $V(t) = V(t+T)$ since $U_1(t)$ is unbiased). In the transformed frame: $i\hbar \partial_t |\psi'(t)\rangle = \hat{H}'(t) |\psi'(t)\rangle$, with $\hat{H}' = \hat{R} \hat{H} \hat{R}^\dagger - i\hbar \hat{R} \frac{d}{dt} \hat{R}^\dagger$. Assuming a fast modulation, $\omega = 2\pi/T \gg J/\hbar, U_0/\hbar$ [1], we integrate the modulation to obtain the effective time-independent Hamiltonian

$$\hat{H}_{\text{eff}} = - \sum_{\langle ij \rangle} \hat{b}_i^\dagger J_{\text{eff}}(\hat{n}_i - \hat{n}_j) \hat{b}_j + \frac{U_0}{2} \sum_i \hat{n}_i (\hat{n}_i - 1), \quad (2)$$

with an effective density-dependent hopping $J_{\text{eff}}(\Delta \hat{n}) = \frac{J}{T} \int_0^T dt e^{iV(t)\Delta \hat{n}}$ in the transformed frame (see Refs. [2, 3] for further details).

We are interested in probing the effective model by TOF measurements. Note, however, that TOF measurements will monitor the evolution of the quasi-momentum distribution in the laboratory frame, $\rho_L(k, t) = \frac{1}{NL} \sum_{l,j} e^{-ik(l-j)} \langle \psi(t) | \hat{b}_l^\dagger \hat{b}_j | \psi(t) \rangle$, with N the number of particles, and L the number of sites. The single-particle correlation function in the laboratory frame

fulfills: $\langle \psi(t) | \hat{b}_i^\dagger \hat{b}_j | \psi(t) \rangle = \langle \psi'(t) | \hat{b}_i^\dagger e^{iV(t)(\hat{n}_i - \hat{n}_j)} \hat{b}_j | \psi'(t) \rangle$, and hence for general times $\rho_L(k, t)$ does not coincide with the quasi-momentum distribution of the effective model $\rho_E(k) = \frac{1}{NL} \sum_{l,j} e^{-ik(l-j)} \langle \psi' | \hat{b}_l^\dagger \hat{b}_j | \psi' \rangle$. We will be interested in stroboscopic measurements at times $t = nT$, with $n = 0, 1, \dots$, such that $\rho_L(k, nT) = \rho_E(k)$. This condition demands $V(0) = 0$, fixing the gauge uncertainty (we assume this gauge fixing henceforth). Hence measurements at times $t = nT$ allow to probe an effective model, \hat{H}_{eff} (see Eq.(2) of the main text). In the following we consider for simplicity $U_1(0) = 0$.

Note that if the modulation starts at time $-T < -t_0 < 0$, $U_1(-t_0) = 0$, then the time evolution between $t = -t_0$ and $t = 0$ must be explicitly considered, i.e. the initial condition for the time evolution under the effective model is $|\psi'(0)\rangle = \mathcal{T} e^{-i \int_{-t_0}^0 \hat{H}'(t') dt'} |\psi(-t_0)\rangle$, where \mathcal{T} denotes time ordering. The discrete time evolution at times nT may be then evaluated, in a very good approximation for $\hbar\omega \gg U_0, J$, by evolving with \hat{H}_{eff} starting with the calculated $|\psi'(0)\rangle$. Note, however, that the measurements will probe a different effective model, due to the different (shifted) form of $U_1(t)$, and hence of $V(t)$, and in turn of $J_{\text{eff}}(\Delta \hat{n})$.

For a sinusoidal modulation $U_1(t) = \tilde{U}_1 \sin(\omega t)$, $V(t) = \frac{\tilde{U}_1}{\omega} [1 - \cos(\omega t)]$, and hence $J_{\text{eff}}(\Delta \hat{n}) = J e^{i\Omega \Delta \hat{n}} J_0(\Omega \Delta \hat{n})$, with $\Omega = \tilde{U}_1/\hbar\omega$ and J_0 the Bessel function of first kind. The stroboscopic measurement of $\rho_L(k, nT)$ allows hence to probe $\rho_E(k)$ for an effective model with a complex $J_{\text{eff}}(\Delta \hat{n}) = |J_{\text{eff}}(\Delta \hat{n})| e^{i\phi(\Delta \hat{n})}$, with a quantum Peierls phase $\phi(\hat{n}_i - \hat{n}_j) = \Omega(\hat{n}_i - \hat{n}_j)$, dependent on the population difference between nearest sites.

The hopping may hence acquire a density-dependent Peierls phase but it may be gauged out by defining new bosonic operators $\hat{B}_j \equiv e^{-i\Omega \hat{n}_j} \hat{b}_j$. Hence, the complex hopping does not affect the ground-state phase diagram [4]. Moreover, the appearance of this phase does not result in an overall shift of $\rho_E(k)$. This may be understood by realizing that by construction $J_{\text{eff}}(-\Delta \hat{n}) = J_{\text{eff}}(\Delta \hat{n})^*$, and hence $\phi(-\Delta \hat{n}) = -\phi(\Delta \hat{n})$. For an homogeneous superfluid, the number difference between neighboring sites presents quantum fluctuations around a zero mean, and the quantum Peierls phases acquire a stochastic character, varying randomly from bond to bond between positive and negative values. As a result the system experiences an effective decoherence. We illustrate this effect in Fig. A1(a), where we show DMRG results for $\rho_E(k)$. Note that when increasing Ω , $\rho_E(k)$ broadens,

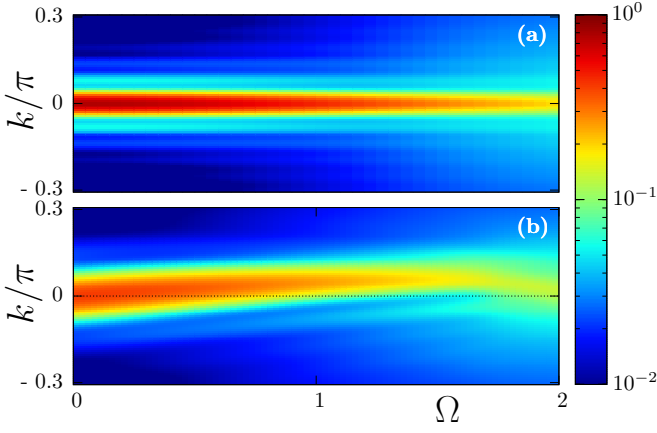


FIG. A1: (a) Quasi-momentum distribution of the ground state of (2) with $J_{\text{eff}}(\Delta\hat{n}) = J e^{i\Omega\Delta\hat{n}} J_0(\Omega\Delta\hat{n})$ as a function of Ω for $\langle\hat{n}\rangle = 1$ and $U_0 = J$. In order to exclude possible superfluid-to-insulator transitions we keep $J/J_0(\Omega)$ constant. (b) Same as (a) but with an on-site energy gradient, $\epsilon \sum_j j n_j$ with $\epsilon = 0.2J$. DMRG calculations [5] were performed in $L = 36$ sites, with a maximal site occupation of 6 bosons.

and may even saturate the Brillouin zone, as a consequence of the dephasing.

A net drift of the quasi-momentum distribution may be however achieved in the presence of a density gradient, which may in turn result from a lattice tilting. Although the created phase still depends on population differences, the density gradient $\langle\hat{n}_j - \hat{n}_{j+1}\rangle \neq 0$ leads to a non-zero average Peierls phase. This is illustrated in Fig. A1(b), where we show that a density gradient results in a net drift of the momentum distribution, in addition to the broadening mentioned above.

B. CREATION OF ARBITRARY DENSITY DEPENDENT PEIERLS PHASES

In the main text the derivation of the AB-model is described for the case $U_{A1}(0 < t < T/2) = -U_{A1}(T/2 < t < T) = \tilde{U}_{A1} \sin(\omega_{AB}t)$ which leads to the density dependent hopping amplitude and phase $\tilde{J}_{AB}(\hat{n}_{2j}) = \frac{J}{2} J_0(\Omega_{AB}\hat{n}_{2j}) e^{i\Omega_{AB}\hat{n}_{2j}} = \tilde{J}_{BA}(\hat{n}_{2j})^*$. So here the phase is always strictly coupled to the modulus of the hopping.

One may choose more generally $U_{A1}(0 < t < T/2) = \tilde{U}_{A1} \sin(\omega_{AB}t + \phi_1)$ and $U_{A1}(T/2 < t < T) = \tilde{U}_{A1} \sin(\omega_{AB}t + \phi_2)$. Note that $\phi_1 = 0$, $\phi_2 = \pi$ reproduces the case shown in figure 1 of the main text. The effective tunneling is given by $\tilde{J}_{AB}(\hat{n}_{2j}) = \frac{J}{2} J_0(\Omega_{AB}\hat{n}_{2j}) e^{i\Omega_{AB} \cos(\phi_1)\hat{n}_{2j}}$ and $\tilde{J}_{BA}(\hat{n}_{2j}) = \frac{J}{2} J_0(\Omega_{AB}\hat{n}_{2j}) e^{i\Omega_{AB} \cos(\phi_2)\hat{n}_{2j}}$. A unitary gauge transformation $b_{2j}^\dagger \rightarrow b_{2j}^\dagger e^{-i(\Phi_{AB} + \Phi_{BA})/2\hat{n}_{2j}}$ may be used to obtain $\tilde{J}_{AB}(\hat{n}_{2j}) = \frac{J}{2} J_0(\Omega_{AB}\hat{n}_{2j}) e^{i\Phi/2\hat{n}_{2j}} = \tilde{J}_{BA}(\hat{n}_{2j})^*$ in Eq. (4) of the main text. Hence, $\Phi =$

$\Phi_{AB} - \Phi_{BA} = \Omega_{AB}[\cos(\phi_1) - \cos(\phi_2)]$ may be changed keeping the hopping modulus unaffected as in Fig. 3(b) of the main text.

C. STRONGLY INTERACTING LIMIT

In the following we discuss briefly the physics in the limit of strong interactions, $U \rightarrow \infty$. As described in the main text, in this limit one can reduce the description to the manifold of 0 and 1 particles per site and introduce an effective spin- $\frac{1}{2}$ Hamiltonian $\hat{H}_{1/2}$ in perturbation theory up to second order J/U as given in the main text. This Hamiltonian may be rewritten as

$$\begin{aligned} \hat{H}_{1/2} = & -J \sum_j [\hat{S}_j^+ \hat{S}_{j+1}^- + \text{h.c.}] \\ & + J_c \sum_j [\hat{S}_j^+ \left(\frac{1}{2} + \hat{S}_{j+1}^z\right) \hat{S}_{j+2}^- + \text{h.c.}] + \\ & + J_s \sum_j (-1)^j [\hat{S}_j^+ \left(\frac{1}{2} + \hat{S}_{j+1}^z\right) \hat{S}_{j+2}^- + \text{h.c.}] + \\ & + \Delta \sum_j \hat{S}_j^z \hat{S}_{j+1}^z \end{aligned}$$

with coefficients $J_c = \frac{J^2}{U} \frac{1+\Gamma^2}{2}$, $J_s = \frac{J^2}{U} \frac{1-\Gamma^2}{2}$ and $\Delta = -\frac{J^2}{U}(1 + |\Gamma|^2)$. Using the standard bosonization dictionary [6] the continuum limit of this Hamiltonian may be expressed as a sine-Gordon Hamiltonian of the density and phase fluctuations $\theta(x)$ and $\phi(x)$. It is precisely the staggered (next-nearest-neighbor) hopping that introduces at half filling a spin-Peierls like term $\sim \sin 2\phi(x)$ which becomes relevant for Luttinger-liquid parameters $K < 2$. That is why at half filling we observe the immediate opening of band insulator gap for arbitrarily small tunneling J/U which is consistent with our numerical simulations. The $S^z - S^z$ -interaction contributes with $\sim \cos 4\phi(x)$ terms, which are irrelevant for $K > 1/2$.

The opening of a gap may be also understood in an easier way if we just consider the correlated hopping parts $\hat{S}_j^+ \hat{S}_{j+1}^z \hat{S}_{j+2}^-$ of the second order perturbation, since this part may be analytically solved by mapping to free fermions:

$$\begin{aligned} \hat{H}_{1/2}^{\text{sf}} = & -J \sum_j \hat{c}_j^\dagger \hat{c}_{j+1} + J_c \sum_j \hat{c}_j^\dagger \hat{c}_{j+2} + \\ & + J_s \sum_j (-1)^j \hat{c}_j^\dagger \hat{c}_{j+2} + \text{h.c.} \end{aligned}$$

Here one finds the spin-Peierls like band-gap opening $\sim |J_s|$ at half filling.

D. THE TWO PARTICLE SCATTERING PROBLEM

In the following we provide a detailed description of the calculation of the two-particle scattering length for the AB-model as given in Eq.(3) of the main text. A general bosonic two particle state is given by

$$|\Psi_Q\rangle = \left[\sum_x \frac{c_{x,x}}{\sqrt{2}} (b_x^\dagger)^2 + \sum_{x,y>x} c_{x,y} b_x^\dagger b_y^\dagger \right] |0\rangle,$$

$$\begin{aligned} (\epsilon - U)C_0 &= -\sqrt{2}J |\Gamma| \left(D_1 e^{i(Q-\Phi)/2} + C_1 e^{-i(Q-\Phi)/2} \right) \\ (\epsilon - U)D_0 &= -\sqrt{2}J |\Gamma| \left(C_1 e^{iQ/2} + D_1 e^{-iQ/2} \right) \\ \epsilon C_1 &= -\sqrt{2}J |\Gamma| \left(C_0 e^{i(Q-\Phi)/2} + D_0 e^{-iQ/2} \right) - J/2 \left(C_2 e^{-iQ/2} + D_2 e^{iQ/2} \right) \\ \epsilon D_1 &= -\sqrt{2}J |\Gamma| \left(C_0 e^{-i(Q-\Phi)/2} + D_0 e^{iQ/2} \right) - J/2 \left(C_2 e^{iQ/2} + D_2 e^{-iQ/2} \right) \\ \epsilon C_{r \geq 2} &= -J/2 \left(C_{r-1} e^{iQ/2} + C_{r+1} e^{-iQ/2} + D_{r-1} e^{-iQ/2} + D_{r+1} e^{iQ/2} \right) \\ \epsilon D_{r \geq 2} &= -J/2 \left(D_{r-1} e^{iQ/2} + D_{r+1} e^{-iQ/2} + C_{r-1} e^{-iQ/2} + C_{r+1} e^{iQ/2} \right) \end{aligned}$$

The energy of the two scattered particles is given by $\epsilon = -2J \cos(q) \cos(Q/2)$. In order to extract scattering properties we solve this set of equations with the ansatz $C_r = e^{-iqr} + v e^{iqr} + \beta \alpha^r$ and $D_r = e^{-iqr} + v e^{iqr} - \beta \alpha^r$ for $r > 1$. The equations for $r > 2$ can be solved by this ansatz if $2i\alpha \cos(q) \cos(Q/2) = (-1 + \alpha^2) \sin(Q/2)$. We choose $|\alpha| < 1$ and solve the remaining four equations for C_0, D_0, v and β . Since the α part decays exponentially fast, we can extract the scattering length $a = -\lim_{q \rightarrow 0} \partial_q \delta$ with $v = e^{2i\delta}$ which after some algebra results in Eq.(3) of the main text.

E. TIME OF FLIGHT IMAGING

As in recent experiments on shaken lattices [7], the shifted quasi-momentum distribution $\rho_E(k)$, may be detected in TOF experiments. However, as mentioned in the main text, the relation between the quasi-momentum distribution of the effective model and TOF imaging presents some features that differ significantly from the shaken lattice case. Interestingly, since atoms at sites A and B belong to different species, it is actually possible to visualize the quasi-momentum distribution of atoms in state $|1\rangle$ and $|2\rangle$ separately (see Fig. A2). Note that for the B sublattice, $\langle \psi(t) | \hat{b}_{2i+1}^\dagger \hat{b}_{2j+1} | \psi(t) \rangle = \langle \psi' | \hat{b}_{2i+1}^\dagger \hat{b}_{2j+1} | \psi' \rangle$, and hence the quasi-momentum distribution observed in TOF will be exactly the same as that of the effective

where $|0\rangle$ is the vacuum. Due to the conservation of total momentum in the scattering process one can express the amplitudes as $c_{x,x+r} = C_r e^{iQ(x+\frac{r}{2})}$ for x in one of the A sites and $c_{x,x+r} = D_r e^{iQ(x+\frac{r}{2})}$ for $x \in B$. Here $Q = q_1 + q_2$, the total momentum (below we employ $q = (q_1 - q_2)/2$ as the half relative momentum). The Schrödinger equation $\hat{H}_{\text{eff}}^{AB} |\Psi\rangle = \epsilon |\Psi\rangle$ for the two particle problem leads to the following system of coupled equations for the amplitudes C_r and D_r with $\Gamma \equiv \frac{1}{2} J_0(\Omega_{AB}) e^{i\Phi/2}$

model at any time. In contrast, for the A sublattice $\langle \psi(t) | \hat{b}_{2i}^\dagger \hat{b}_{2j} | \psi(t) \rangle = \langle \psi' | \hat{b}_{2i}^\dagger e^{iV(t)(\hat{n}_{2i} - \hat{n}_{2j})/\hbar} \hat{b}_{2j} | \psi' \rangle$. As a result, the quasi-momentum distribution of the A sublattice just coincides with that of the effective model (and also with that of the sublattice B) at times $t = nT$. For intermediate times, the phase appearing in the conversion between both reference frames leads to a broadening, and eventual blurring, of the TOF peaks (Fig. A2). Note that this blurring is in itself a result of the number-dependence of the effective model, being related with the stochastic phase discussed in Sec. A.

F. CORRELATION FUNCTIONS IN THE SUPERFLUID REGIME

In this section we provide additional details concerning the bosonization of the AB model, and the calculation of correlation functions in the SF regime. We consider the Hamiltonian:

$$\begin{aligned} \hat{H}_T &= -\frac{J}{2} \sum_j \left\{ \hat{b}_{2j}^\dagger F[\hat{n}_{2j}] \hat{b}_{2j+1} + \hat{b}_{2j}^\dagger F[\hat{n}_{2j}]^* \hat{b}_{2j-1} + H.c. \right\} \\ &+ \frac{U_0}{2} \sum_j \hat{n}_j (\hat{n}_j - 1), \end{aligned} \quad (3)$$

which becomes the AB model in the main text for $F(x) = \mathcal{J}_0(\Omega_{AB}x) e^{-i\Omega_{AB}x}$. We employ the bosonization: $b_j^\dagger \rightarrow \rho(x_j)^{1/2} e^{-i(\theta(x_j) - \eta x_j)}$, with $\rho(x) \simeq \rho_0 - \frac{1}{\pi} \partial_x \phi$

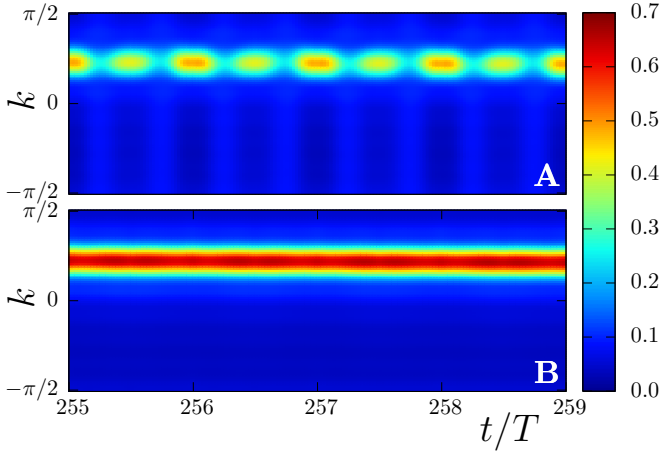


FIG. A2: Quasi-momentum distribution of the A and the B components in the laboratory frame as a function of time for $\langle \hat{n} \rangle = 3/2$ and $\Omega_{AB} = 0.8$, and same parameters as those of Fig.5 of the main text.

(neglecting the contribution of higher harmonics), ρ_0 the average density, and x_j the position of site j . Note the displacement $\eta = \arg[F(\rho_0)]$ that results from the presence of a complex hopping. This displacement is introduced to remove linear terms in $\partial_x \theta$, and leads to an overall drift of the momentum distribution. The Hamiltonian (up to irrelevant constants and terms proportional to $\partial_x \phi$ that may be reabsorbed in the chemical potential) becomes of the form:

$$\hat{H} = \frac{u}{2\pi} \int dx [K^{-1}(\partial_x \phi)^2 + K(\partial_x \theta)^2 + 2\gamma(\partial_x \phi)(\partial_x \theta)], \quad (4)$$

$$F_1(x, \tau) = \frac{1}{2} \ln \left[\frac{(x + i(\chi + u\tau(1 + |\gamma|)))(x - i(\chi + u\tau(1 - |\gamma|)))}{\chi^2} \right] \quad (9)$$

For $\tau \rightarrow 0^+$, and $x \gg \chi$, we obtain $F_1(x) = \ln |x|$, i.e. the dependence found for $\gamma = 0$ [6]. As a consequence the single particle correlation acquires the standard (γ -independent) form: $\hat{b}_i^\dagger \hat{b}_j \sim |i-j|^{1/2K}$. Similarly, one may evaluate the density-density correlation which acquires as well the standard form: $\langle \hat{n}_i \hat{n}_j \rangle = \rho_0^2 - \frac{K}{2\pi^2 x^2}$ (neglecting oscillatory terms).

Note that the arguments above are not specific for the AB model. Any density-dependent hopping would result in a Hamiltonian of the form (4). In particular for the anyon Hubbard model discussed in Ref. [9]: $\hat{H} = -t \sum_j \left\{ \hat{b}_j^\dagger e^{i\alpha \hat{n}_j} \hat{b}_{j+1} + H.c. \right\} + \frac{U_0}{2} \sum_j \hat{n}_1(\hat{n}_j - 1)$, one

where in the weak-coupling regime:

$$\frac{uK}{2\pi} = \frac{J\rho_0}{2} \tilde{F}(\rho_0), \quad (5)$$

$$\frac{u}{2\pi K} = \frac{U_0}{2\pi^2} - \frac{J}{2\pi^2} \mathcal{R} \left[\rho_0 \frac{d^2 \tilde{F}(\rho_0)}{d\rho^2} + 2 \frac{d\tilde{F}(\rho_0)}{d\rho} \right], \quad (6)$$

$$\frac{u\gamma}{2\pi} = -\frac{J\rho_0}{2\pi} \mathcal{I} \left[\frac{d\tilde{F}(\rho_0)}{d\rho} \right], \quad (7)$$

with \mathcal{R} (\mathcal{I}) the real (imaginary) part. Note that $\gamma \neq 0$ only if the hopping is density-dependent and complex, i.e. in the presence of a density-dependent gauge field.

In the strong-coupling regime the particular relation between the microscopic parameters and the coefficients of the low-energy Hamiltonian may be modified, but the form of the bosonized Hamiltonian (4) is preserved. We may hence evaluate correlation functions using the standard formalism, see e.g Ref. [6].

In particular, $\langle (\phi(x, \tau) - \phi(0, 0))^2 \rangle = KF_1(x, \tau)$ (with τ the imaginary time) and $\langle (\theta(x, \tau) - \theta(0, 0))^2 \rangle = K^{-1}F_1(x, \tau)$, where (introducing a cut-off length χ that may be equated to the lattice spacing):

$$F_1(x, \tau) = \frac{1}{2\pi} \int_{-\infty}^{\infty} dk e^{-\chi|k|} \int_{-\infty}^{\infty} d\omega \frac{1 - \cos(kx - \omega u\tau)}{k^2 + (\omega - i\gamma k)^2}. \quad (8)$$

Note that compared to the expression with $\gamma = 0$ [6], the only effect of the mixing term $(\partial_x \phi)(\partial_x \theta)$ consists in a frequency shift $\omega \rightarrow \omega - i\gamma k$. For $|\gamma| < 1$ [8]

obtains in the weakly-interacting regime:

$$K^2 = \frac{\pi^2}{\alpha^2 + \frac{U_0}{2\rho_0 t}}, \quad (10)$$

which, as shown in Fig. A3 matches very well with our numerical results for $\rho_0 = 0.25$ and $U_0 = t$. Note that in this case a density-dependent Peierls phase, without any associated decrease of the hopping strength, results as well in a non-trivial decay of K .

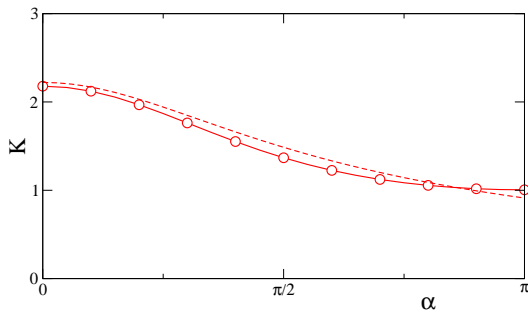


FIG. A3: Dependence of the Luttinger parameter K as a function of α for the anyon model of Ref. [9], for $\rho_0 = 0.25$ and $U_0 = t$. The circles denote our numerical results obtained from DMRG calculations of the single-particle correlation function, whereas the dashed line depicts the analytical curve (10).

G. DETAILS OF THE NUMERICAL SIMULATION OF REAL TIME EVOLUTIONS

For the dynamical calculations of Fig. 5 of the main text, and Fig. A2 we have used TEBD[10] calculations for 16 sites with up to 300 states, and a maximal site occupation of 4 bosons. As in Ref. [11], we may simulate rather long evolution times ($t \sim 400T$) due to the quasi-adiabatic character of the dynamics. We have carried out our TEBD simulations for time steps $dt = T/400$ and $m = 300$ matrix states, which compare well to simulations with $dt = T/600$ and $m = 400$, showing the convergence of the results. Smaller system sizes, with a correspondingly decreased ramping and evolution time, display very similar behavior and error-bars. The non-adiabaticity of the finite ramping time leads to oscillations in the expectation value of k_{max} after the ramping procedure. The time-average and standard deviation are shown as points and error-bars in Fig. 5 of the main text and compare very well to the ground-state expectation.

be necessary. In order to avoid photon-assisted inter-band transitions, the modulation frequency must be sufficiently small compared to the energy gap $\hbar\Delta_{GAP}$ to the first excited band. Considering a sinusoidal modulation $U_1(t) = \tilde{U}_1 \sin(\omega t)$, for an amplitude $\Omega \equiv \tilde{U}_1/\hbar\omega = 2$, $\omega = \Delta_{GAP}/10$ ($\Delta_{GAP} \simeq 10$ kHz) would be necessary (A. Rapp and L. Santos, in preparation), whereas for weaker modulations larger modulation frequencies may be employed, but always avoiding multi-photon resonances.

- [2] J. Gong, L. Morales-Molina and P. Hänggi, *Phys. Rev. Lett.* **103**, 133002 (2009).
- [3] Á. Rapp, X. Deng, and L. Santos, *Phys. rev. Lett.* **109**, 203005 (2012).
- [4] More involved modulations of the interactions may lead in general to a Peierls phase which is not linear in the number difference, but in general an odd function. The momentum distribution will hence show a stochastic broadening rather than a net drift, as for the linear case. Moreover, the cubic part of the phase is only relevant when the modulus of the hopping is very small, due to the large argument of the Bessel function. It has hence negligible consequences in the ground-state phase diagram.
- [5] U. Schollwöck, *Annals of Physics* **326**, 96 (2011).
- [6] *Quantum Physics in one dimension*, Th. Giamarchi, Oxford University Press, 2004.
- [7] J. Struck *et al.*, *Phys. Rev. Lett.* **108** 225304 (2012).
- [8] For the AB model (and also the anyon model of Ref. [9]) $|\gamma| < 1$ within the weak-coupling regime. A value $|\gamma| > 1$ would lead to $F_1(x, \tau) = 0$, and hence to non-decaying correlations. In all our numerical calculations single-particle correlations present a polynomial decay with a finite power, and hence $|\gamma| < 1$ in all our calculations, also in the strong-coupling limit.
- [9] T. Keilmann, S. Lanzmich, I. McCulloch, and M. Roncaglia, *Nature Commun.* **2**, 361 (2011).
- [10] G. Vidal, *Phys. rev. Lett.* **91**, 147902 (2003).
- [11] D. Poletti and C. Kollath, *Phys. Rev. A* **84**, 013615 (2011).

[1] For typical values of J and U_0 of the order of 10 to 100 Hz, a modulation of several 100 Hz to 1 kHz would